Int. J. Heat Mass Transfer. Vol. 30, No. 9, pp. 1941–1948, 1987
Printed in Great Britain

0017–9310/87 $3.00 + 0.00
© 1987 Pergamon Journals Ltd.

Natural convection and radiation heat transfer from staggered vertical fins

G. GUGLIELMINI, E. NANNEI and G. TANDA
Dipartimento di Ingegneria Energetica, Universita' di Genova, via all'Opera Pia 15a, 16145 Genova, Italy

(*Received* 21 *February* 1986 *and in final form* 2 *September* 1986)

Abstract—The heat transfer by natural convection and radiation between an isothermal vertical surface, having a staggered array of discrete vertical plates of finite thickness, and the surroundings is investigated. The natural convection contribution has been measured for several geometric configurations with low emittance surfaces, analysing the influence of the most significant parameters. The radiant component has been evaluated by applying the configuration factor algebra to all the surfaces of the system, assumed isothermal, diffuse and gray. The theoretical results have been experimentally verified by measuring the exchanged heat flux through surfaces of known emissivity. For the particular geometry taken into account, the convective and radiant components yield a more efficient heat transfer than that obtained from fins made up of U-shaped vertical channels of the same bulk volume.

1. INTRODUCTION

MANY TECHNIQUES have been introduced in the past years to improve the efficiency of heat exchange systems involving natural convection and/or forced convection, and with or without phase change [1]. In this area of research, Sparrow and Prakash [2] have considered heat transfer enhancement in natural convection using an array of discrete plate segments in lieu of a continuous uninterrupted surface. Their study was aimed at reducing the thermal boundary layer thickness in order to obtain higher heat transfer coefficients. Therefore, short vertical elements were considered to prevent a thermally developed boundary layer. The degree of enhancement and the related conditions have been evaluated in ref. [2] by numerical analysis applied to the study of a two-dimensional system. The results are expressed as a function of two parameters: the number of plates in a subchannel formed by two adjacent columns and the ratio between the interspace of the plates and the height of the whole system. Within the range of values examined the greatest improvement was by a factor of two.

Whereas Sparrow and Prakash [2] analysed a two-dimensional problem assuming the plates to be infinitely long in the third dimension, a more practical situation would involve an array of parallel vertical plates having one edge connected to a vertical wall. Also, unlike the thin plate assumption made in ref. [2], the plate fins would actually have some finite thickness. The aim of this paper is to investigate this more realistic situation; i.e. the task is to study the heat exchange from vertical staggered plates of finite length and thickness, connected to an isothermal baseplate. Figure 1 shows the finned surface examined in this paper.

In addition to natural convection, the analysis also accounts for radiation which can have a significant contribution to the total heat exchange. The convective component was experimentally evaluated, on a wide range of geometrical parameters. The radiant heat flux was calculated by means of the finned surface shape factor (towards the surroundings) obtained by an analytical scheme.

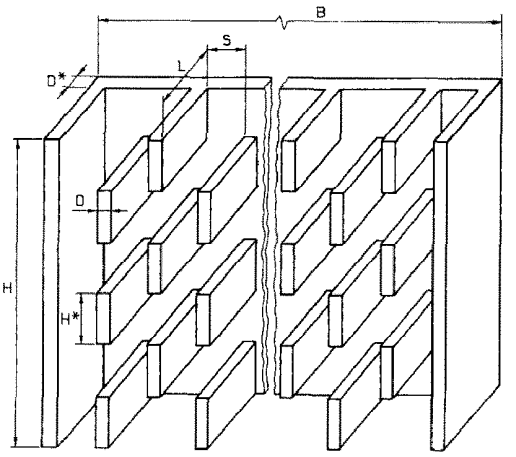

FIG. 1. Finned heat sink configuration with staggered array of discrete plates.

The results have been used to determine the geometrical configuration to optimize the heat flux for a finned surface at a given bulk volume.

2. BACKGROUND

No correlation of natural convection for channels delimited by staggered arrays of discrete vertical plates attached to a perpendicular baseplate has been found in the available literature. The bibliography dealing with analytical and experimental studies carried out on systems of parallel vertical plates is instead much richer.

NOMENCLATURE

a channel aspect ratio, S/L
A overall heat transfer surface of the heat sink [m^2]
$\bar{A}$ total area of elements having shape factor equal to 1 [m^2]
A_c area of a repetitive discrete plate channel [m^2]
A^* area of an end side channel [m^2]
B overall test width [m]
c_1–c_6 coefficients in equation (1)
c_p specific heat at constant pressure [J kg^{-1} K^{-1}]
C_c, C_i conductance by convection and radiation for a finned surface with a staggered array of discrete vertical plates [W K^{-1}]
$\hat{C}_c$, $\hat{C}_i$ conductance by convection and radiation for a finned surface made up of U-shaped vertical channels [W K^{-1}]
D fin thickness [m]
D^* fin base thickness [m]
$F_{w,z}$ shape factor from w surface to z surface
$F_{c,\infty}$, $F^*_{c,\infty}$, $F_{A,\infty}$ shape factor of a repetitive channel, end side channel and whole staggered finned surface towards ambient environment
$\hat{F}_{c,\infty}$ shape factor of U-shaped channel towards ambient environment
g acceleration of gravity [m s^{-2}]
Gr_H Grashof number $g\beta(T_A-T_\infty)H^3/\nu^2$
Gr_r Grashof number, $g\beta(T_A-T_\infty)r^3/\nu^2$
$\bar{h}$ average heat transfer coefficient [W m^{-2} K^{-1}]
H overall height of finned surface [m]
H^* height of discrete plates [m]
L fin length [m]
M overall height to discrete plate height ratio, H/H^*
N total number of channels
Nu_H Nusselt number, $\bar{h}H/\lambda$
Nu_r Nusselt number, $\bar{h}r/\lambda$
P thermal power, q_i+q_c [W]
Pr Prandtl number, $c_p\mu/\lambda$
q_c heat transfer rate by convection [W]
q_i heat transfer rate by radiation [W]
r characteristic length, $2LS/(L+S)$ [m]
Ra_r Rayleigh number, $Gr_r Pr$
Ra_r^* modified Rayleigh number, $(r/H)Ra_r$
S transverse spacing across two adjacent columns of discrete vertical plates [m]
T_A, T_∞ surface and ambient environment absolute temperature [K]
V constant in equation (1), -929.14 m^{-1}
x_j j-surface forming an enclosure [m^2].

Greek symbols

β volumetric coefficient of expansion [K^{-1}]
ε radiation emissivity
Φ_1, Φ_2 functions in equation (1)
λ thermal conductivity [W m^{-1} K^{-1}]
μ dynamic viscosity [kg m^{-1} s^{-1}]
ν kinematic viscosity [m^2 s^{-1}]
ψ function in equation (1)
σ 5.67×10^{-8} W K^{-4} m^{-2}.

Elenbaas [3] has obtained a relation for vertical plates by solving the boundary layer equations. Aibara [4] has shown that for U-shaped finned surfaces, the heat exchange by natural convection is essentially the same as for the parallel plate channel of infinite length. Such an approximation leads to a less than 5% error in the heat transfer rate only when the ratio of channel depth to channel width is greater than 5. Van de Pol and Tierney [5] have developed a semiempirical correlation for U-shaped channels fitting the experimental data from twelve fin arrays. Their relationship can also be used for channels with relatively short depth.

As already mentioned, a numerical analysis for an isothermal staggered array of discrete vertical plates of infinite length along the horizontal direction has been performed in ref. [2]. However, as stated before, the results obtained cannot be applied to the geometry dealt with in this paper because the influence of the normal baseplate, as well as the length and finite thickness of the fin are not taken into account. Suzuki *et al.* [6] have numerically and experimentally studied a system made of a staggered array of vertical flat plates in mixed convection at low Reynolds numbers considering the finite thickness of the segments, but again, the problem is different than the one examined in this paper.

3. ANALYSIS

3.1. *Convective heat transfer*

The geometrical configurations considered in refs. [2–5] may be regarded as limiting cases of the one shown in Fig. 1 when some geometrical parameters approach limit values. Hence a relationship has been developed so as to approximate the solutions of the most important limit cases including the one studied in ref. [2]. After the structure of the correlation has been defined, numerical coefficients were evaluated using the experimental data obtained from twelve aluminum finned surfaces of low emittance ($\varepsilon = 0.05$). The modified Rayleigh number Ra_r^* varied from 65 to 500 and the characteristic length r from 0.96×10^{-2} to 1.56×10^{-2} m.

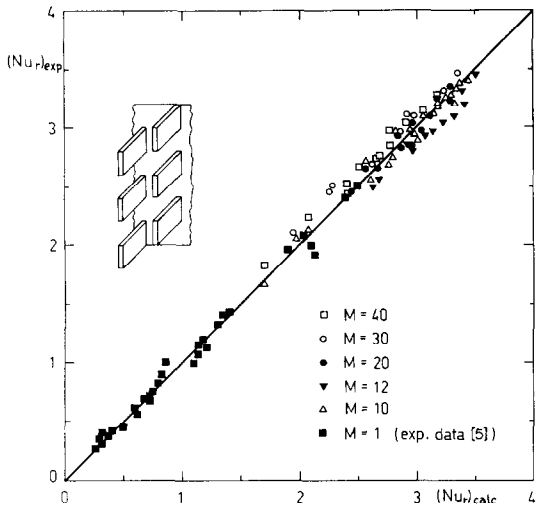

FIG. 2. Comparison of experimental and calculated Nusselt number.

The relationship was obtained assuming a constant temperature for the whole surface and a constant ambient fluid temperature (taken equal to 20°C).

The relationship expressed as a Nusselt number is as follows:

$$Nu_r = \frac{Ra_r^*}{\psi\Phi_1}\{1-\exp[-\psi\Phi_2(0.5/Ra_r^*)^{0.75}]\} \quad (1)$$

where

$$\Phi_1 = 1+\{1-\exp[-(10/M)^{0.15}]\} \cdot \exp(-c_1 a^{c_2} M^{c_3}) \ln M$$

$$\Phi_2 = 1+1.67\{1-\exp[-1.9(10/M)^{0.15}]\} \cdot \exp(-c_4 a^{c_5} M^{c_6}) \ln M$$

$$\psi = 24[1-0.483\exp(-0.085/a)]/\{[1+a][1+[1-\exp(-1.66a)] \cdot [12.926a^{0.5}\exp(VS)-0.61]]\}^3$$

$$c_1 = 5, \quad c_2 = 0.5, \quad c_3 = 0.06$$
$$c_4 = 1.74, \quad c_5 = 0.08, \quad c_6 = 0.165$$
$$V = -929.14\ \text{m}^{-1}.$$

All thermophysical properties are evaluated at the wall temperature, except for the β value, calculated at the fluid temperature.

Equation (1) allows the experimental data for a staggered finned surface with a 4% standard deviation to be correlated (Fig. 2) and it is valid for other geometrical configurations representing limit cases.

For U-shaped channels characterized by $M = 1$ and by a distance between adjacent fins equal to the double of the S term in equation (1), the function ψ is equal to that defined in ref. [5] while Φ_1 and Φ_2 approach unity. As a consequence equation (1) becomes identical to the one defined in ref. [5], provided that the aspect ratio a is based on the quantity S depicted in Fig. 3(c).

For a system made of parallel plates of infinite length ($M = 1$, $L \to \infty$) equation (1) yields

$$Nu_r = \frac{Ra_r^*}{24}\{1-\exp[-24(0.5/Ra_r^*)^{0.75}]\}$$

which is Elenbaas' parallel flat plate solution [3], where $r = 2S$ (for $L \to \infty$) is the characteristic length equal to the distance between two adjacent plates of infinite length. Figure 3 shows the definition assumed for geometrical parameters (S, M) varying the configuration of the channel.

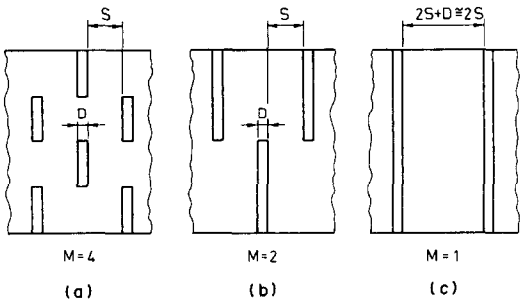

FIG. 3. Definition of geometrical parameters varying the configuration of the channel.

When a staggered array of discrete vertical plates of infinite length ($M > 1$, $L \to \infty$) is considered, equation (1) becomes

$$Nu_r = \frac{Ra_r^*}{24\Phi_1}\{1-\exp[-24\Phi_2(0.5/Ra_r^*)^{0.75}]\}$$

where

$$\Phi_1 = 1+\{1-\exp[-(10/M)^{0.15}]\}\ln M$$

$$\Phi_2 = 1+1.67\{1-\exp[-1.9(10/M)^{0.15}]\}\ln M$$

which approximates to within $\pm 5\%$ the numerical results obtained in ref. [2] for a similar configuration, provided the different definition of characteristic length in ref. [2] and in this paper is taken into account.

If the fin length approaches zero, equation (1) becomes, for any M value

$$Nu_H = 0.595 Ra_H^{0.25}$$

which approximates to within 1% of McAdams' relation for natural convection on vertical isothermal plates [7].

In conclusion, equation (1) allows, with good accuracy, the mean convective heat transfer coefficient to be evaluated for an array of vertical plates, either continuous or discrete, attached to a baseplate, by varying the geometrical parameters. The relationship does not take into account the plate thickness; however the effect of this parameter is negligible in the range of $D/S < 0.3$ and it is consistent with ref. [6].

3.2. *Radiation heat transfer*

The evaluation of the radiant heat flux between finned surface and surroundings was performed with the configuration factor algebra [8] assuming the heat sink surface to be isothermal, gray and diffuse. At first, a repetitive channel divided into a finite number

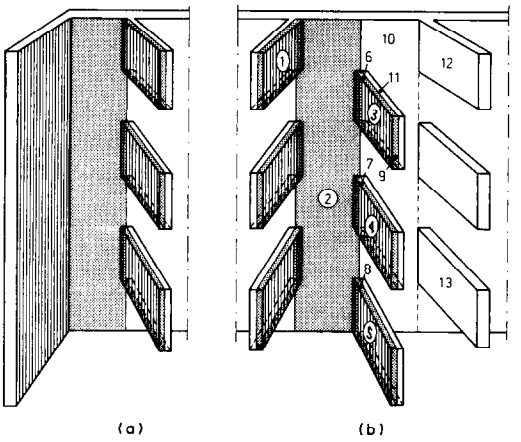

FIG. 4. End side channel (a) and repetitive channel (b).

of simple geometry elements was defined for the whole surface, shown in Fig. 4(b). The shape factor between each channel and the environment was calculated, taking the environment to be at a constant temperature and characterized by absorptance equal to 1. Referring to the surface of the side element shown in Fig. 4(b) under number 1, the shape factor is given as follows:

$$F_{1,\infty} = 1 - F' - F''$$

where $F' = F_{1,2} + F_{1,3} + F_{1,4} + F_{1,5} + F_{1,6} + F_{1,7} + F_{1,8}$ is the shape factor from surface 1 to the surfaces of the reference channel and $F'' = F_{1,10} + F_{1,11} + F_{1,12} + F_{1,13}$ is, with good accuracy, the shape factor from surface 1 to the surfaces outside of the channel but parts of the heat sink. Since a fraction of energy emitted from surface 1 towards surfaces 10 and 13 impinges on surfaces 3–8, the evaluation of F'' is quite laborious.

The same procedure has been applied to all the other components of elementary geometry such as surface 2 of the baseplate between two arrays of segments, side surfaces 3, 4, 5, etc. of the segments and surfaces 6, 7, 8, 9, etc. arising due to the finite plate thickness.

The shape factor $F_{c,\infty}$ (with respect to the environment) of the repetitive channel was obtained combining the single shape factors as shown in the appendix.

Figure 5 shows the calculated results for the repetitive channel using a computer program. The shape factor is given as a function of the H/L ratio between the overall height of the array and the fin length, for different values of the parameters M and L/S, where S is the transverse spacing across a channel. The results were obtained by assuming the ratio D/H^* between the thickness and the height of the single segment equal to 0.2, S/H^* ranging from 0.4 to 2. The shape factor $F_{c,\infty}$ increases with decreasing L/S. At constant L/S, the shape factor $F_{c,\infty}$ is affected by the lowest

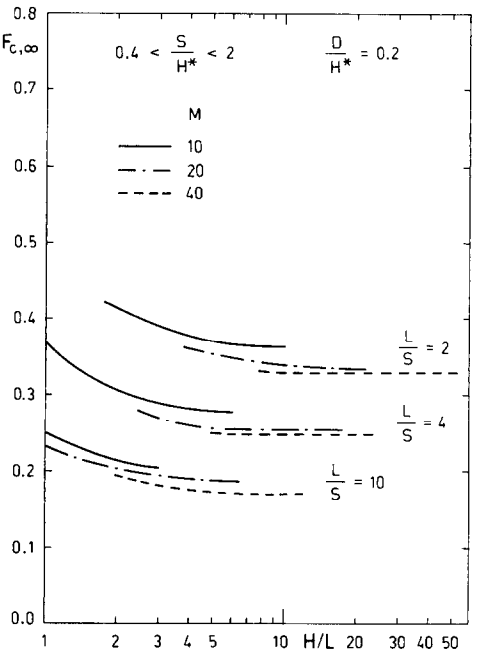

FIG. 5. Repetitive channel shape factor.

values of H/L while M is not significant in the explored range.

The results for the channel can be extended with good accuracy to the whole finned surface except for the external channels bounded by an array of rectangular segments and by the continuous side plate shown in Fig. 4(a). The contribution of the two end side channels to the radiant heat transfer diminishes as the number of channels N increases. As a consequence, a good guess for $F^*_{c,\infty}$ is to take a mean value of the shape factors $F_{c,\infty}$ of the repetitive and $\hat{F}_{c,\infty}$ of the U-shaped channels having the same overall height, H, depth L and interspace between plates S. $\hat{F}_{c,\infty}$ can be evaluated either by the same procedure used for the discrete plate repetitive channel or by the results presented in refs. [9, 10].

The total radiant heat exchange q_i can be obtained from $F_{c,\infty}$ and $F^*_{c,\infty}$ and from the radiative properties of the material of the heat sink, as shown in the appendix. The final relationship, which includes all contributions to heat exchange of the whole extended surface, is as follows:

$$q_i = \frac{\varepsilon F_{A,\infty}}{1-(1-\varepsilon)(1-F_{A,\infty})} A\sigma(T_A^4 - T_\infty^4) \qquad (2)$$

where the quantities are defined in the appendix.

4. EXPERIMENTAL RESULTS AND DISCUSSION

In order to compare the analytical approach developed for the evaluation of the radiant heat flux and determine the numerical coefficients (c_1–c_6) in equation (1), many experiments have been carried out on extended surfaces of different dimensions (Table

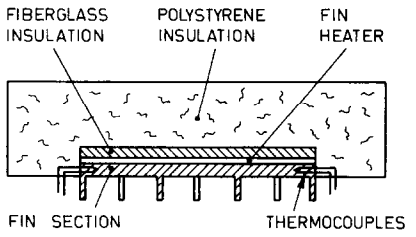

FIG. 6. Test fin apparatus (section).

1). The first set of experiments (S1) was made on finned coated surfaces (black anodized) of high emissivity. The second one (S2) was performed on the same specimens having mirror polished surfaces. The third one (S3) was carried out using the specimens of set S2, replacing the original end metal sides with vertical low conductivity plates of the same dimensions. The experiments were performed on the apparatus shown in Fig. 6, which displays a section of the fin baseplate assembly. The finned surfaces were made of aluminum (for its high thermal conductivity and for the ease of coating) to yield a timewise-invariant high emissivity value. The heat sink baseplate was heated by an electrical plane heater placed on its back and insulated by means of a 5 mm fibreglass layer. The fin baseplate-assembly was inserted in a block of 70 mm thick polystyrene. The average temperature of the heat sink was measured by means of six thin chromel–alumel thermocouples placed inside 0.5 mm holes in the plate base. Since fin efficiency has resulted close to unity, the measured temperature values were assumed for the whole finned surface. Air temperature was measured by a shielded thermocouple to prevent thermal radiation between the thermocouple and the environment. Tests were carried out in an enclosed room (at $20 \pm 0.5°C$) to provide a still atmosphere by varying the thermal heat flux without exceeding an 80°C surface temperature of the heat sink.

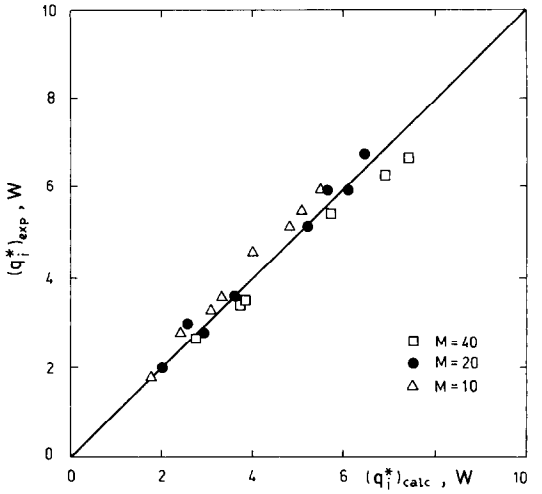

FIG. 7. Comparison of experimental and calculated radiant heat transfer rates.

4.1. *Radiant component*

The radiant component was evaluated by means of the experiments S1 and S2. The emissivity values of the finned surfaces, measured by an experimental apparatus [11], were 0.85 and 0.05, respectively. For each specimen the two sets of experiments, carried out at the same surface temperature, make it possible to eliminate the convective contribution and check equation (2), the difference of the overall heat transfer being equal to the difference (q_i^*) between the radiant fluxes.

Figure 7 shows a comparison between the experimental values $(q_i^*)_{exp}$ and $(q_i^*)_{calc}$ from equation (2), for extended surfaces at different temperatures. The results agree with an 8% standard deviation.

4.2. *Convective component*

The mean convective component of the baseplate and the staggered array of discrete vertical plates was

Table 1. Test fin dimensions

Configuration number	Fin height H (m)	Overall width B (m)	Fin length L (m)	Transverse spacing across a channel S (m)	Fin thickness D (m)	Fin base thickness D^* (m)	H/H^* ratio M
1	0.075	0.11	0.020	0.0063	0.002	0.005	10
2	0.075	0.11	0.020	0.0063	0.002	0.005	12
3	0.075	0.11	0.035	0.0063	0.002	0.005	10
4	0.075	0.11	0.035	0.0063	0.002	0.005	12
5	0.150	0.11	0.020	0.0078	0.002	0.005	10
6	0.150	0.11	0.020	0.0078	0.002	0.005	20
7	0.150	0.11	0.035	0.0078	0.002	0.005	10
8	0.150	0.11	0.035	0.0078	0.002	0.005	20
9	0.300	0.11	0.020	0.0100	0.002	0.005	30
10	0.300	0.11	0.020	0.0100	0.002	0.005	40
11	0.300	0.11	0.035	0.0100	0.002	0.005	30
12	0.300	0.11	0.035	0.0100	0.002	0.005	40

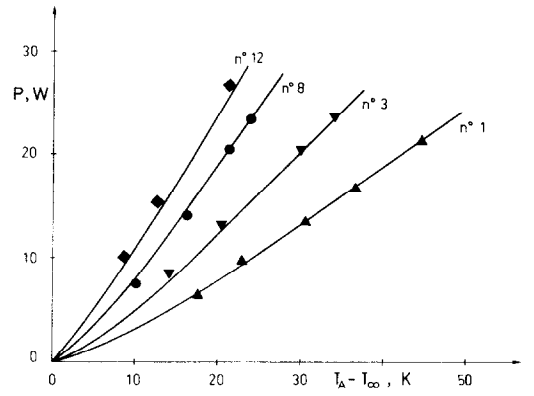

FIG. 8. Comparison of experimental and analytical heat transfer rates.

evaluated by using mirror polished extended surfaces ($\varepsilon = 0.05$). The influence of the continuous end sides was minimized using vertical low conductivity plates in lieu of the original end metal sides (experiments S3). The radiant contribution, evaluated by equation (2) with $\varepsilon = 0.05$, was subtracted by the measured heat flux and the results were used in fixing the constants c_1–c_6 in equation (1).

4.3. *Combined natural convection and radiation heat transfer*

The reliability of the method used for analysing the heat transfer due to natural convection and radiation from the whole finned surface has been verified by means of the experiments (S1) on heat sinks (see Fig. 1) having black anodized surfaces ($\varepsilon = 0.85$).

The heat transfer by natural convection from the baseplate and from the staggered array can be computed by equation (1). With reference to the two end continuous sides, the mean heat transfer coefficients on the inside and the outside can be evaluated by the relation suggested in refs. [5, 7], respectively. The radiant heat transfer from the whole finned surface can be determined by equation (2).

By means of the convective and radiant components, it is possible to evaluate the total heat flux dissipated at a given temperature rise above ambient. Such a procedure was applied, as an example, to type 1, 3, 8, 12 surfaces (Table 1) of 0.85 emissivity. Figure 8 shows the good accuracy resulting from the comparison of the experimental and theoretical values.

For these extended surfaces radiation ranges from 40 to 25% of the total heat dissipated (P), $T_A - T_\infty$ varying from 10 to 50°C in agreement with experimental and analytical results presented in ref. [12] for highly populated pin fin arrays. At higher rise temperatures, the contribution of radiant heat flux increases.

Once the calculation procedure has been verified, it is possible to compare the predicted thermal conductance of the extended surfaces analysed here and that of surfaces made of U-shaped vertical channels.

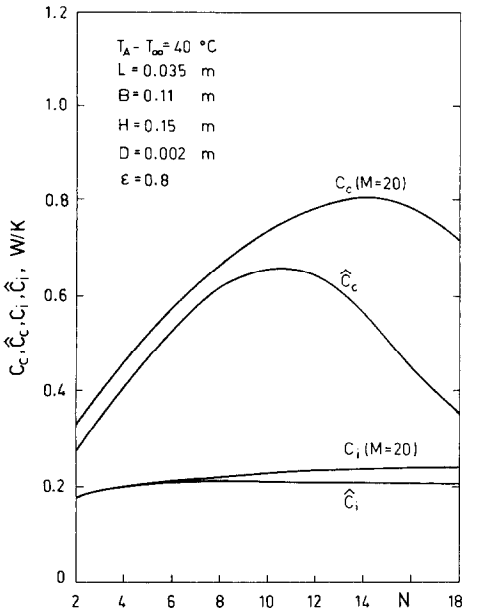

FIG. 9. Thermal conductances of heat sinks, with continuous or discrete vertical plates, vs number of channels.

Such a comparison may be performed either at the same heat transfer surface, as pointed out in ref. [2] for natural convection from a staggered array of infinite length discrete plates, or at the same bulk volume of the heat sink. The latter condition seems more interesting because the sink volume is often the relevant parameter in the application of refrigeration of electronic components.

By holding external dimensions (L, B and H) fixed, it is possible to compare the convective and radiant thermal conductance for heat sinks made of vertical continuous and discrete plates (at fixed M). The calculation results of convective (C_c discrete plates, $\hat{C}_c$ continuous plates) and radiant conductances (C_i discrete plates, $\hat{C}_i$ continuous plates) are presented in Fig. 9 with N channels on the abscissa. In spite of the heat transfer surface reduction, the finned surface with staggered discrete plates yields greater thermal conductance than the U-shaped one. Furthermore, owing to the reduction of the thermal boundary layer, a consequence of the breaking of the continuous vertical plates, the maximum convective conductance corresponds to higher values of N.

5. CONCLUDING REMARKS

An investigation on the heat flux exchange by natural convection and radiation from a finned surface made of a staggered array of discrete vertical plates has been performed. The experiments, carried out on systems of different geometrical dimensions, allowed a correlation for natural convection which provides the mean convective heat transfer coefficient for an array of vertical plates, continuous or discrete, connected to a vertical baseplate. The radiant component has

been studied applying the configuration factor algebra. The calculation results presented by graphs agree with good accuracy with experimental data obtained on different emissivity surfaces. The calculation procedure of the total heat flux exchanged is consistent with the experimental heat transfer characteristic of the heat sink studied here.

At the same bulk volume, the comparison between conductances of heat sinks made of U-shaped channels and a staggered array of discrete plates shows higher thermal performance for the latter which more than compensates for the reduced area. Of considerable interest is the utilization of this particular heat sink in the cooling of electronic equipment.

REFERENCES

1. A. E. Bergles, Survey and evaluation of techniques to augment convective heat and mass transfer, *Prog. Heat Mass Transfer* **1**, 331–424 (1969).
2. E. Sparrow and C. Prakash, Enhancement of natural convection heat transfer by a staggered array of discrete vertical plates, *J. Heat Transfer* **102**, 215–220 (1980).
3. W. Elenbaas, Heat dissipation of parallel plates by natural convection, *Physica* **9**, 1–28 (1942).
4. T. Aibara, Natural convective heat transfer in vertical parallel fins of rectangular profile, *Jap. Soc. Mech. Engng* **34**, 915–926 (1968).
5. D. W. Van de Pol and J. K. Tierney, Free convection Nusselt number for vertical U-shaped channels, *J. Heat Transfer* **95**, 542–543 (1973).
6. K. Suzuki, E. Hirai, T. Miyake and T. Sato, Numerical and experimental studies on a two-dimensional model of an offset-strip-fin type compact heat exchanger used at low Reynolds number, *Int. J. Heat Mass Transfer* **28**, 823–836 (1985).
7. W. H. McAdams, *Heat Transmission*, p. 172. McGraw-Hill, New York (1954).
8. R. Siegel and J. R. Howell, *Thermal Radiation Heat Transfer*. McGraw-Hill, New York (1981).
9. S. N. Rea and S. E. West, Thermal radiation from finned heat sinks, *IEEE Trans.* **12**, 115–117 (1976).
10. G. N. Ellison, *Thermal Computations for Electronic Equipment*. Van Nostrand Reinhold, New York (1984).
11. R. Bartolini, C. Isetti and E. Nannei, On the effect of annealing on total normal emittance of oxidized steel, *Int. J. Heat Mass Transfer* **28**, 309–311 (1985).
12. E. M. Sparrow and S. B. Vemuri, Natural convection/radiation heat transfer from highly populated pin fin arrays, *J. Heat Transfer* **107**, 190–197 (1985).

APPENDIX

Consider a finned surface composed of n finite areas x_j ($j = 1, n$) forming an enclosure with a hypothetical surface x_∞ simulating the ambient environment.

The following restrictions are met:

(a) all radiant energy is emitted and reflected diffusely;

(b) the absolute temperatures T_A of each area x_j ($j = 1, n$) and T_∞ of ambient x_∞ are constant and uniform.

Under these assumptions, reciprocity relations and configuration factor algebra give

$$\left(\sum_{j=1}^{k} x_j\right) F_{(1+2+\cdots+k),\infty} = x_\infty F_{\infty,(1+2+\cdots+k)} \tag{3}$$

$$x_\infty F_{\infty,(1+2+\cdots+k)} = x_\infty F_{\infty,1} + x_\infty F_{\infty,2} + \cdots + x_\infty F_{\infty,k} \tag{4}$$

$$x_\infty F_{\infty,1} + x_\infty F_{\infty,2} + \cdots + x_\infty F_{\infty,k} = x_1 F_{1,\infty} + x_2 F_{2,\infty} + \cdots + x_k F_{k,\infty} \tag{5}$$

with $k \leqslant n$.

By using equations (3)–(5) the shape factor $F_{c,\infty}$ from a channel to the environment is

$$F_{c,\infty} = \frac{\sum_{j=1}^{m} x_j F_{j,\infty}}{A_c} \tag{6}$$

where A_c is the whole area of the channel, x_j and $F_{j,\infty}$ are the area and the shape factor of jth element of the channel (divided into m elements).

Equations (3)–(5) can be applied to compute the shape factor $F_{A,\infty}$ from an extended surface with staggered discrete plates to the ambient environment

$$F_{A,\infty} = \frac{(N-2)A_c F_{c,\infty} + 2A_c^* F_{c,\infty}^* + \bar{A}}{(N-2)A_c + 2A_c^* + \bar{A}}. \tag{7}$$

$F_{c,\infty}$ and $F_{c,\infty}^*$ are the shape factors of the repetitive channel shown in Fig. 4(b) and of the end side channel shown in Fig. 4(a), evaluated by equation (6); A_c and A_c^* represent the corresponding heat transfer surfaces. N is the number of channels and $\bar{A}$ the external surface of the two lateral continuous sides, having shape factor equal to 1.

Obviously it must be

$$\sum_{j=1}^{n} x_j = \bar{A} + 2A_c^* + (N-2)A_c = A$$

where A is the overall heat transfer surface of the device.

Since A and x_∞ form an enclosure, with the hypothesis of diffuse and gray surfaces, it follows that:

$$q_i = \frac{\sigma(T_A^4 - T_\infty^4)}{(1-\varepsilon)/(A\varepsilon) + 1/(AF_{A,\infty}) + (1-\varepsilon_\infty)/(x_\infty \varepsilon_\infty)} \tag{8}$$

where σ is the Stefan–Boltzmann constant, ε and ε_∞ finned surface and environment emissivity, T_A and T_∞ the respective absolute temperatures, while $F_{A,\infty}$ is computed by equation (7). If the emissivity of the ambient environment is 1, equation (8) becomes

$$q_i = \frac{\varepsilon F_{A,\infty}}{1-(1-\varepsilon)(1-F_{A,\infty})} A\sigma(T_A^4 - T_\infty^4)$$

where q_i is the net heat transfer by radiation exchanged between the finned surface A and the ambient environment.

CONVECTION NATURELLE ET RAYONNEMENT THERMIQUE POUR DES AILETTES VERTICALES ESPACEES

Résumé—On étudie le transfert thermique par convection et rayonnement entre une surface isotherme verticale ayant un arrangement de plaques verticales discrètes, d'épaisseur finie et l'environnement. La contribution de la convection naturelle a été mesurée pour différentes configurations géométriques avec des surfaces à faible émittance, en analysant l'influence des parmètres les plus actifs. La part de rayonnement a été évaluée en appliquant l'algèbre de facteur de configuration à toutes les surfaces du système, supposées isothermes, diffuses et grises. Les résultats théoriques ont été expérimentalement vérifiés en mesurant le flux de chaleur à travers des surfaces d'émissivité connue. Pour la géométrie particulière considérée, les composantes de convection et de rayonnement donnent un transfert thermique plus efficace que pour des ailettes à canaux verticaux en forme de U et de même volume.

WÄRMEÜBERGANG DURCH NATÜRLICHE KONVEKTION UND STRAHLUNG VON VERSETZT ANGEORDNETEN VERTIKALEN RIPPEN

Zusammenfassung—Dar Wärmeübergang durch natürliche Konvektion und Strahlung zwischen einer isothermen senkrechten Oberfläche, die mit einem versetzten Feld von einzelnen senkrechten Blechen endlicher Dicke versehen ist, und der Umgebung wird untersucht. Der Anteil der natürlichen Konvektion wurde für mehrere geomtrische Anordnungen mit Oberflächen niedriger Emission gemessen, wobei der Einfluß der bedeutsamsten Parameter analysiert wird. Der Strahlungsanteil wurde durch die Anwendung der Algebra der Sichtfaktoren auf alle Oberflächen des Systems, die als isotherm, diffus-reflektierend und grau angenommen wurden, ermittelt. Die theoretischen Ergebnisse wurden durch die Messung der Wärmestromdichte an Oberflächen von bekanntem Emissionsgrad experimentell bestätigt. Für die in Betracht gezogene besondere Geometrie erbringen die Konvektions- und Strahlungsanteile einen besseren Wärmeübergang als bei Rippen, die aus U-förmigen vertikalen Kanälen gleichen Volumens bestehen.

СВОБОДНО-КОНВЕКТИВНЫЙ И ЛУЧИСТЫЙ ТЕПЛООБМЕН ОТ ВЕРТИКАЛЬНЫХ РЕБЕР, РАСПОЛОЖЕННЫХ В ШАХМАТНОМ ПОРЯДКЕ

Аннотация—Исследован свободно-конвективный и лучистый теплообмен между изотермической вертикальной поверхностью, на которой в шахматном порядке расположены дискретно вертикальные пластины конечной толщины, и окружающей средой. Измерен вклад свободной конвекции для нескольких геометрических конфигураций с поверхностями, имеющими низкую излучательную способность, с учетом влияния наиболее существенных параметров. С помощью алгебры формпараметров, примененной для всех поверхностей, которые считались изотермическими, диффузными и серыми, определена лучистая компонента. Результаты теоретических расчетов подтверждены данными измерений теплового потока через поверхности с известной лучепоглощательной способностью. Найдено, что для рассмотренной геометрии конвективная и лучистая компоненты обеспечивают более интенсивный теплообмен, чем у ребер, образованных U-образными вертикальными каналами при тех же среднеобъемных значениях.